Design Modifications to SMX Static Mixer for Improving Mixing

Shiping Liu, Andrew N. Hrymak, and Philip E. Wood
Dept. of Chemical Engineering, McMaster University, Hamilton, Ontario L8S 4L7, Canada

DOI 10.1002/aic.10608
Published online October 24, 2005 in Wiley InterScience (www.interscience.wiley.com).

Laminar mixing in SMX static mixers and the effect of geometry on mixing are studied using computational fluid dynamics. A frame-indifferent parameter is used to classify the flow types in the SMX mixer. All three typical flows (simple shear, pure elongation, and squeezing) appear within the flow field of the SMX mixer. The strain rate distribution in the SMX mixer is observed to be very nonuniform. A mixing element with 10 crossbars shows the best mixing quality, followed closely by the standard SMX mixing element with eight crossbars. The improved designs of the mixing element increase the average and peak strain rate, and provide a more uniform strain rate distribution and faster mixing rate compared to those of the standard SMX mixer. © 2005 American Institute of Chemical Engineers *AIChE J,* 52: 150–157, 2006
Keywords: laminar flow, mixing, flow type, SMX static mixer, computational fluid dynamics

Introduction

Static mixers have been applied for continuous laminar mixing of viscous liquids in many chemical industry applications, such as polymer processing, polymerization reactions, food processing, paints, pharmaceuticals, and water treatment. Static mixers usually consist of a number of identical motionless mixing elements placed in a pipe or channel. The elements are usually rotated 90° relative to the neighboring elements because this periodic change in the geometry of static mixers produces reorientation and redistribution of the fluids. The SMX static mixer is an important class of static mixer in these applications.

The SMX static mixing elements (Sulzer Chemtech, Winterthur, Switzerland) consist of crossed bars at a 45° angle with the axis of the round pipe. Each element is rotated 90° with respect to the previous element. A standard SMX mixing element has eight crossbars and an aspect ratio of length to diameter $l/D = 1$. SMX static mixers are observed to exhibit a fast mixing rate and relatively modest pressure drop. Previous authors have also labeled other arrangements of crossbar mixers with larger aspect ratio or square cross section as SMX static mixers.[1-3]

Previous experimental works investigated pressure drops and concentration distributions in SMX static mixers. The usual measure of pressure drop is the ratio k of the pressure drop in the static mixer (ΔP_{SM}) to the pressure drop in the empty tube (ΔP_0), which is constant at low Reynolds number.[4-6]

Computational fluid dynamics (CFD) was used to study flow and mixing in SMX static mixers in round tubes and pipes.[7-11] All these CFD simulations were limited to the existing geometry of SMX static mixers and did not investigate the influence of the change in geometry on pressure and mixing. Only a few publications involve a change in geometry in SMX type static mixers in a square duct. Mickaily-Huber et al.[12] found that 90 ° inner tube crossing angles provides the most efficient mixing in the SMRX static mixer. A smaller crossing angle reduces the pressure drop but makes mixing worse. Visser et al.[3] simulated flow and heat transfer in an SMX static mixer in a square duct for mixing elements with two, four, and eight crossbars. However, their study was focused on comparing a two-crossbar geometry with a four-crossbar geometry in heat transfer, and only pressure drop and velocity components were compared in

Correspondence concerning this article should be addressed to A. N. Hrymak at hrymak@mcmaster.ca.

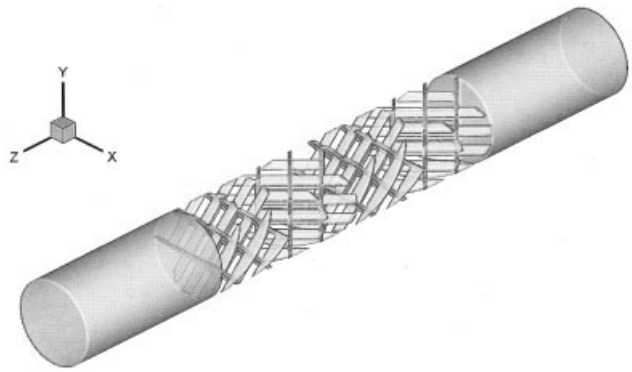

Figure 1. Geometry of standard SMX static mixer with eight crossbars.

all three geometries. In addition, in the simulations of Visser et al.[3] only one mixing element was used in the mesh geometry. The computed velocity profile at the beginning of the element was rotated 90° and then used as inflow profile for the second mixing element and so on for more subsequent elements. Such a treatment of the flow domain totally ignored the transition between two elements and did not give adequate flow fields.

In this article, characteristics of the flow field in a standard SMX static mixer (strain rate distribution and flow type) were investigated. In addition, static mixer design parameters such as the effect of the crossbar number (or equivalently bar width) of the mixing element design on mixing and pressure drop were studied and some new designs, with a reduced mixer element aspect ratio, were proposed.

Characteristics of Flow Field in Standard SMX Static Mixer

The standard SMX mixer element studied in this work has eight crossbars, a diameter of 52 mm, and crossbar thickness of 2 mm. The aspect ratio *l*/*D* is 1. The crossbar width next to the tube wall is 8 mm, whereas the others are 6 mm.

Three-dimensional (3-D) simulations of the steady laminar flows of incompressible Newtonian fluid in the SMX static mixer were carried out using the commercial CFD software FLUENT 5 (Fluent Inc., Lebanon, NH). The mesh geometry with four mixing elements (Figure 1) was produced using GAMBIT (Fluent Inc.). The *z*-axis is the axis of the tube, with the origin at the beginning of the first mixer element, and its direction is the predominant flow direction. The inlet section and outlet section are two empty tubes of 2-D length, to provide a developmental flow length consistent with the inlet and outlet boundary conditions. A fully developed flow velocity profile is applied to the inlet of the mixer and the no-slip boundary condition is applied on the tube walls and mixer element surfaces. A constant pressure outlet condition ($P = 0$) is used. The mesh has a total of 2,217,698 tetrahedral elements and 433,463 nodes, with a nominal cell size of 1 mm in mixer section and 2 mm in inlet and outlet sections. The density and viscosity of Newtonian fluid are 846 kg/m^3 and 1 Pa·s, respectively. The average flow velocity is 0.01 m/s, resulting in a Reynolds number of 0.44. Experiments show that flow in the SMX static mixer is laminar under Re < 10.[4,5] Therefore, the given flow condition is within the typical laminar flow range.

A second-order pressure interpolation scheme is used, with second-order upwinding for the convective terms, and the SIMPLE algorithm for pressure–velocity coupling. The termination tolerance is a normalized residual error of 10^{-5}. Computation time is on the order of 1.5 h using 16 CPUs on SGI Origin 2000.

Strain rate distribution

Strain rate is an important parameter for mixing, especially for dispersive mixing, and is defined as $\dot{\gamma} = \sqrt{2(\mathbf{D} : \mathbf{D})}$, where **D** is the rate of deformation tensor. Figure 2 shows the strain rate distributions at several cross-sectional planes in the first mixing element. The strain rate distribution in the SMX mixer is very nonuniform. High strain rate zones are located around the crossbars. A relatively small strain rate appears in the cross sections where crossing bars are sparse. The strain rate is very low within certain cross sections and this low level of strain rate provides poor dispersive mixing.

Flow types

Simple shear flow and elongational flow show different mixing behavior and efficiency. The orientation of an infin-

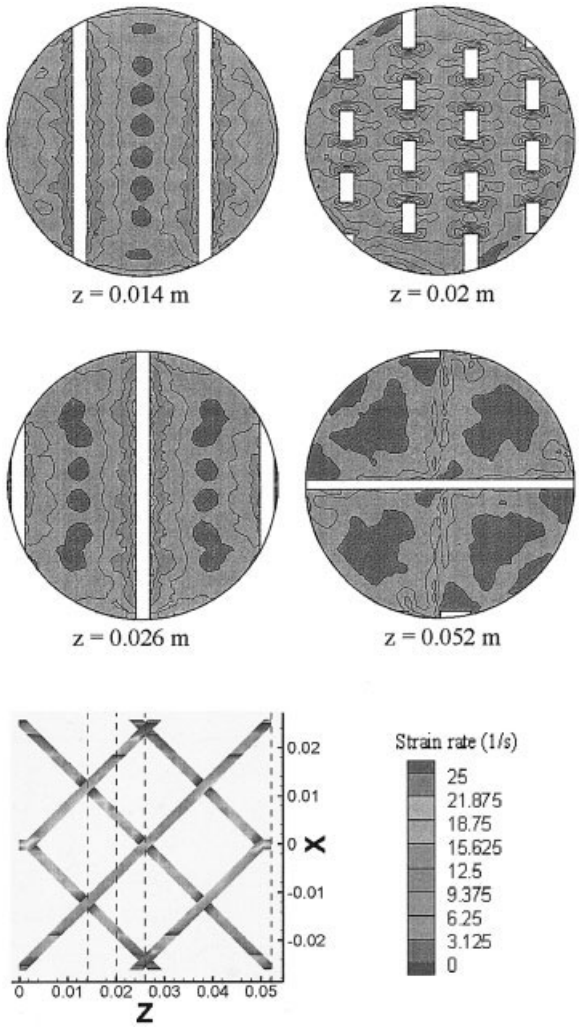

Figure 2. Contours of strain rate on cross sections in the first element of SMX mixer.

itesimal filament in axisymmetric extensional flow always tends to be at the optimum direction to reach the maximum specific rate of stretching, whereas the orientation of an infinitesimal filament in simple shear flow always tends to be parallel to streamlines to make the specific rate of stretching equal to zero. Therefore, elongational flow is more efficient than simple shear flow for mixing. Unfortunately, classification of flow types in a complicated three-dimensional geometry is not simple. The parameter used to judge flow types must be frame indifferent.

Ottino[13] defined the frame-indifferent instantaneous stretching efficiency e_λ as

$$e_\lambda = \frac{D \ln \lambda / Dt}{(\mathbf{D} : \mathbf{D})^{1/2}} \tag{1}$$

where λ is the length stretch and $\mathbf{D}$ is the rate of deformation tensor.

Because $\mathbf{D}$ is symmetric, there always exist three mutually perpendicular principal directions (eigenvectors of $\mathbf{D}$) along which the specific rate of stretching $D \ln \lambda/Dt$ has a maximum and a minimum value.[14] If λ_i and $\mathbf{n}_i$ are the eigenvalues and eigenvectors of $\mathbf{D}$, respectively, where $\lambda_1 > \lambda_2 > \lambda_3$, $D \ln \lambda/Dt$ has the maximum value λ_1 when the line orientation is the eigenvector $\mathbf{n}_1$, and the minimum value of $D \ln \lambda/Dt$ is λ_3 when the line orientation is the eigenvector $\mathbf{n}_3$. It is clear that demixing occurs when the line orientation is the eigenvector $\mathbf{n}_3$. Equation 1 can be rewritten as[15]

$$e_\lambda = \frac{D \ln \lambda / Dt}{\lambda_1} \frac{\lambda_1}{(\mathbf{D} : \mathbf{D})^{1/2}} \tag{2}$$

When the line orientation is the eigenvector $\mathbf{n}_1$, stretching efficiency e_λ reaches its maximum value

$$e_{\lambda\,\max} = \frac{\lambda_1}{(\mathbf{D} : \mathbf{D})^{1/2}} \tag{3}$$

Therefore, for axisymmetric extensional flows, $e_{\lambda\,\max} = \sqrt{2/3} \approx 0.816$; for squeezing flows, $e_{\lambda\,\max} = \sqrt{1/6} \approx 0.408$; and for two-dimensional flows such as simple shear flow, $e_{\lambda\,\max} = \sqrt{2}/2 \approx 0.707$. We use the maximum stretching efficiency $e_{\lambda\,\max}$ to classify the flow types in the SMX static mixer.

The rate of deformation tensor $\mathbf{D}$ and its eigenvalues are derived from the velocity field obtained from the computational fluid dynamics (CFD) results. Figure 3 gives the velocity vectors and contours of $e_{\lambda\,\max}$ on the cross-sectional planes at $z = 0.01$ and 0.02 m in the SMX mixer. The values of $e_{\lambda\,\max}$ indicate that all three typical flows (simple shear, pure elongation, and squeezing) appear within the flow field of the SMX mixer. Velocity vectors show that flow is convergent when $e_{\lambda\,\max} \cong 0.8$ and flow is divergent when $e_{\lambda\,\max} \cong 0.4$. Convergent and divergent flows are natural characteristics of elongational and squeezing flows for incompressible fluids, respectively. The "X" shape of crossbars produces the elongational and squeezing flows. The elongational flow is located at the upstream of the cross-points, whereas the squeezing flow is located at the downstream of the cross-points.

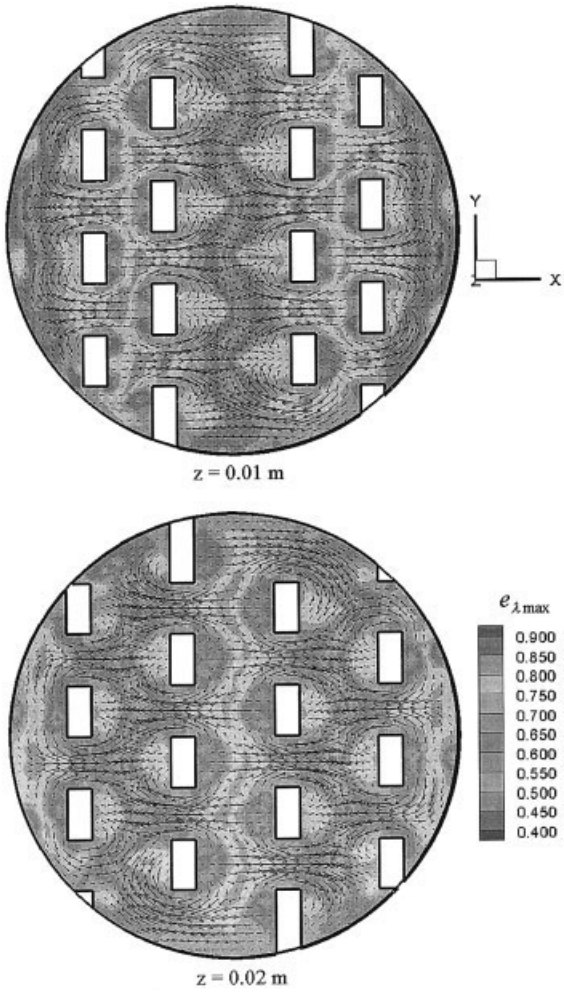

Figure 3. Velocity vectors (including *x*, *y*, *z* components) and contours of $e_{\lambda\,\max}$ on cross sections in the first element of standard SMX mixer.

Effect of Crossbar Number on Mixing and Pressure Drop

The modified mixer geometries maintain the other standard SMX design parameters: 45 ° angle with the axis of the pipe, an aspect ratio of 1, and the thickness of crossbars and the diameter of the tube are also the same as given above. Flow conditions are kept the same as previously described. Seven different mixer element geometries are studied: 4, 6, 8, 10, 12, 16, and 18 crossbar elements. Figures 4 and 5 show SMX-like mixer element geometries with 4 and 16 crossbars, respectively.

The velocity vectors on the cross section at $z = 0.01$ m for crossbar numbers 4, 8, and 16 are given in Figure 6, where the gray-scale contours are for the magnitudes of $\sqrt{v_x^2 + v_y^2}$, that is, the projection of the velocity vector on the cross-sectional plane. The area-weighted average magnitudes of $\sqrt{v_x^2 + v_y^2}$ for crossbar numbers 4, 8, and 16 are 0.0092, 0.0067, and 0.0051 m/s, respectively. Fewer crossbars (or equivalently wider bars)

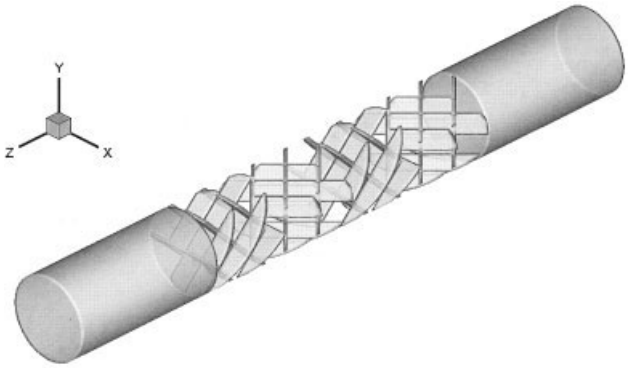

Figure 4. Geometry of SMX mixing elements with four crossbars.

show larger radial velocity components, which improve radial mixing and the overall rate of mixing.

Figure 7 shows the area-weighted average strain rate on cross sections in the first element for each design case. Figure 8 gives pressure drop ratios for all cases and, as expected, those designs with higher crossbar number show greater shear rate and pressure drop.

Figure 9 shows a histogram of the maximum stretching efficiency, $e_{\lambda\,\max}$, for crossbar numbers of 4, 8, and 16. The relative volume fractions of $e_{\lambda\,\max}$ in the mixer sections are calculated, that is, the volumes of the empty tubes in the inlet and outlet section are not included. The relative volume fractions of $e_{\lambda\,\max} \geq 0.775$ for crossbar numbers 4, 8, and 16 are 11.8, 11.4, and 6.7%, respectively. The relative volume fractions of $0.675 \leq e_{\lambda\,\max} \leq 0.725$ for crossbar numbers 4, 8, and 16 are 32.7, 27.9, and 36.7%, respectively. Therefore, the mixing element with a crossbar number of 16 has a lower volume fraction dominated by elongational flow and a comparatively higher volume fraction with shear flow than the mixing elements with crossbar numbers of 4 and 8.

Particle tracking is used to indicate the effect of crossbar number on distributive mixing, with 20,000 particles uniformly distributed in a circle of radius of 1 mm centrally injected at the inlet plane. Numerical integration is performed using a fixed spatial increment rather than a fixed time step; a spatial increment value of 0.1 mm is chosen and 30,000 integration steps are taken. The spatial increment of 0.1 mm is about 10% of the

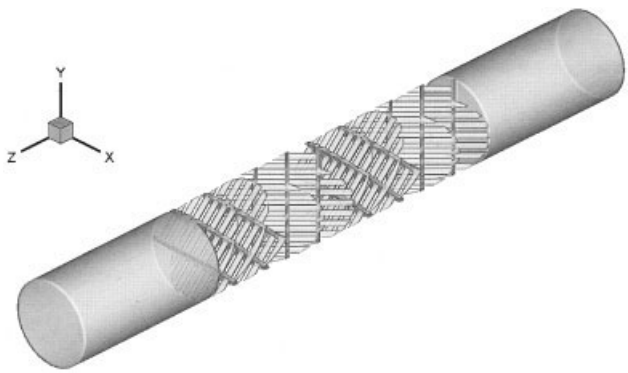

Figure 5. Geometry of SMX mixing elements with 16 crossbars.

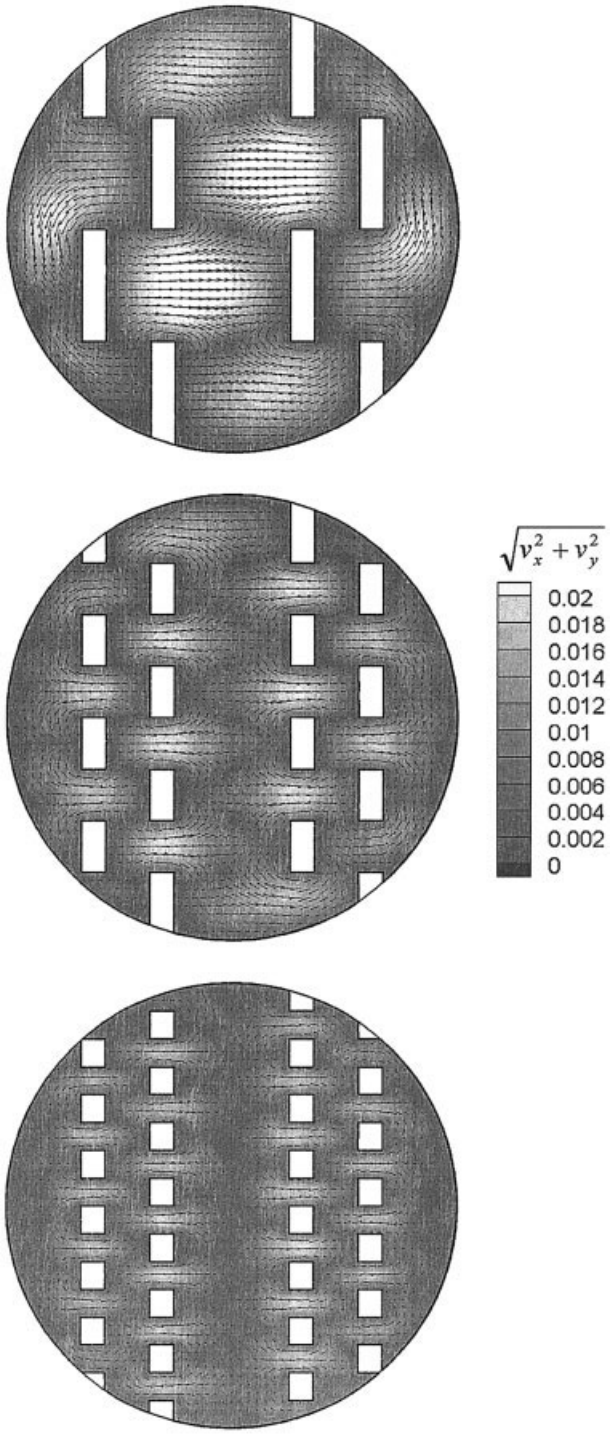

Figure 6. Velocity vectors and contours of $\sqrt{v_x^2 + v_y^2}$ on the cross sections at $z = 0.01$ m for crossbar numbers 4, 8, and 16.

minimum normal cell size. Such spatial increment in integration gives very good agreement with the laser-induced fluorescence (LIF) experiment.[16] The particles are tracked through the static mixer and their positions are recorded when the particles traverse the cross-sectional planes at the end of each element, as shown in Figure 10. When the crossbar number is >10,

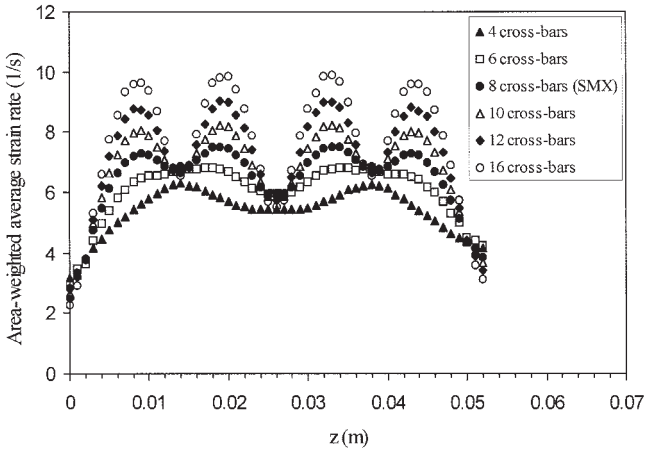

Figure 7. Area-weighted average strain rate on cross sections in the first element for different crossbar numbers.

mixing becomes much worse than those cases with a smaller crossbar number, as a consequence of decreased magnitude of the radial velocity components.

A statistical method is used to quantitatively describe and compare the mixing quality from the particle tracking for different geometries in Figure 10. The cross-sectional flow area at the end of each mixer element is divided into $N = 1916$ small squares of 1×1 mm. The number of particles within each sample square is counted. The particle concentration c_i is the particle number in the ith square. If $c_i = 0$, the ith square is blank with no tracer particles. The coefficient of variation (COV) is usually used to evaluate the degree of mixing[17]:

$$COV = \frac{\sigma}{\bar{c}} \tag{4}$$

where

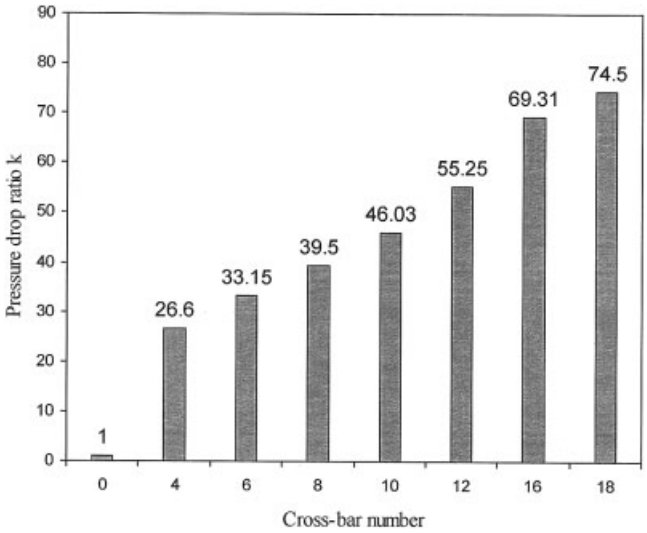

Figure 8. Pressure drop ratio vs. crossbar number.

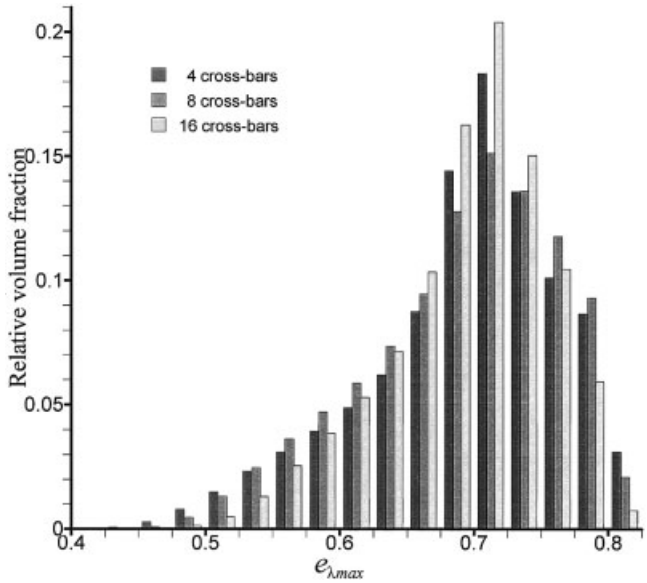

Figure 9. Histogram of the maximum stretching efficiency $e_{\lambda\,max}$ for different crossbar numbers.

$$\bar{c} = \frac{1}{N}\sum_{i=1}^{N} c_i \tag{5}$$

$$\sigma = \sqrt{\frac{1}{N}\sum_{i=1}^{N} (c_i - \bar{c})^2} \tag{6}$$

The significance of the *COV* is that the smaller its value, the more homogeneous the particle distribution. The COV is shown in Figure 11. A crossbar number 10 shows the best particle distribution with the smallest *COV* in the last two elements among all seven geometries. A crossbar number 8 shows the second-best mixing.

Effects of Aspect Ratio

Two modified mixer geometries in which the aspect ratio *l*/*D* of mixing elements is <1 were examined for their mixing characteristics compared with those of the standard SMX mixer. The two modified geometries and the standard SMX mixer are given in Figure 12. The width and thickness of crossbars as well as crossing angle of crossbars of the new mixing elements are the same as those of the standard SMX mixing element, but crossbars are rearranged and the new elements have smaller aspect ratios. The first mixer modification (Figure 12a) has six mixing elements with an aspect ratio of 2/3, whereas the second mixer modification (Figure 12b) has eight elements with an aspect ratio of 1/2. The standard SMX static mixer has four mixing elements with an aspect ratio of 1 (Figure 12c). Thus, the three static mixers have the same total length of $4D$ in the mixing section.

The modified mixer elements have a denser arrangement of crossbars than that of the standard SMX mixer. Figure 13 shows that both new designs increase the average and peak strain rate as well as making the strain rate distribution more

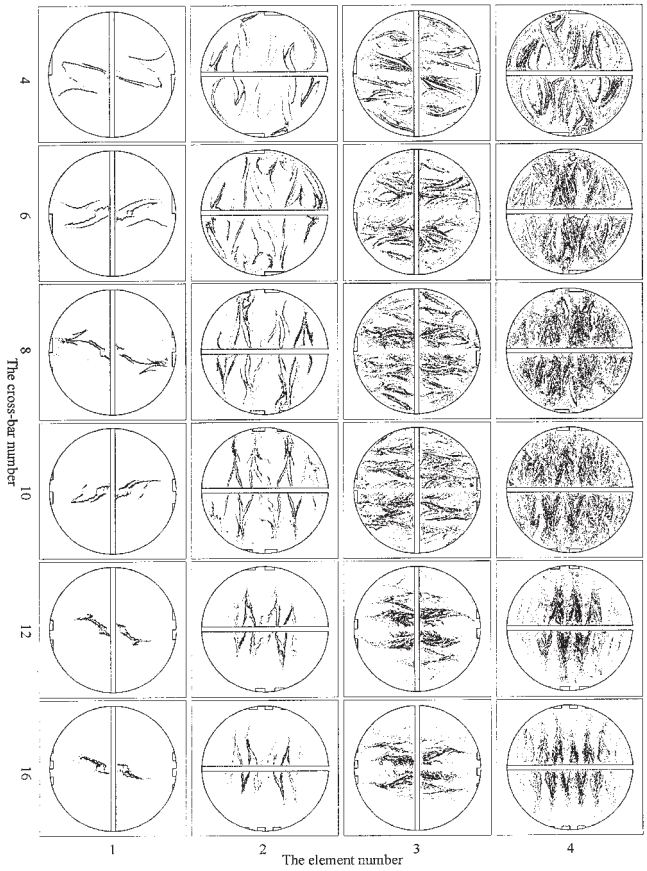

Figure 10. Particle distributions through the mixers with central feeding of 20,000 tracers for mixing elements with different crossbar number.

From the first row to the sixth row, crossbar number is 4, 6, 8, 10, 12, and 16; from the first column to the fourth column, element number is 1, 2, 3, and 4.

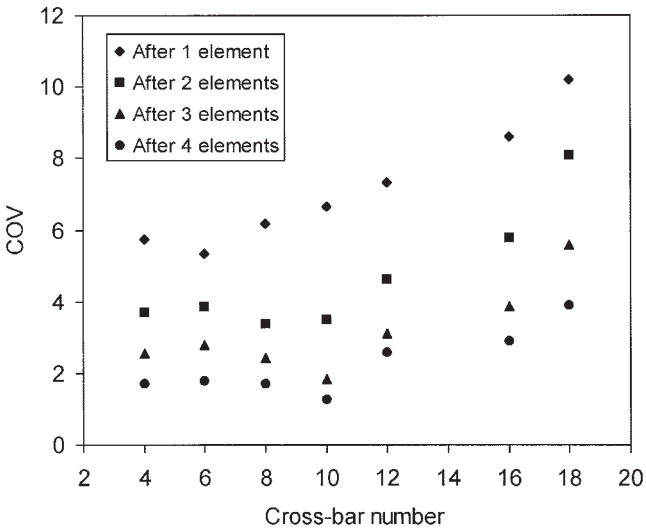

Figure 11. Coefficient of variance with increasing element number for different crossbar numbers.

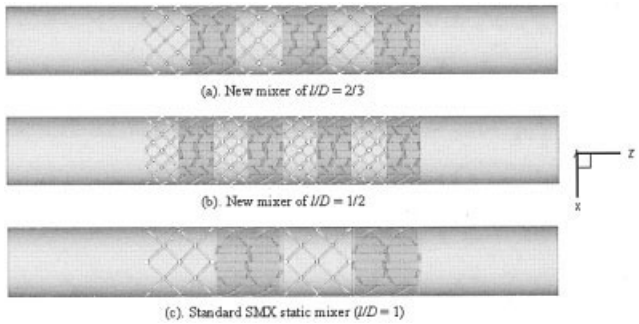

Figure 12. New designs of static mixers.

uniform than the standard SMX mixer. The ratios of the pressure drop in static mixer to the pressure drop in an empty tube for the standard SMX static mixer, the new mixer of $l/D = 2/3$, and the new mixer of $l/D = 1/2$ are $k = 39.5$, 74.7, and 126.1, respectively.

Mixing quality is visualized by particle tracking, where 20,000 particles are centrally injected at the inlet uniformly distributed in a circle of radius of 1 mm. The positions of particles (Figure 14) are recorded when particles intersected the planes at $z = 0.104$ and 0.22 m (12 mm after the last mixing element). The cross-sectional areas at $z = 0.22$ are divided into 2008 small squares of 1×1 mm. The particle concentration, that is, the number of particles within each sample square, is counted. Standard deviation σ and the mean $\bar{c}$ of concentrations are obtained. The coefficients of variation (COV) for standard SMX mixer, the new mixer of $l/D = 2/3$, and the new mixer of $l/D = 1/2$ are 1.67, 0.86, and 0.83, respectively. The mixer elements with reduced aspect ratio exhibit a lower value of COV than that of the standard SMX mixer in the same average mixing time (that is, fixed mixer length). Therefore, the rate of mixing is improved in the proposed geometries, compared to that in the standard SMX design. It is noticed that the new mixer of $l/D = 1/2$ does not show a significantly higher COV than that of the new mixer of $l/D = 2/3$. More particle tracers and

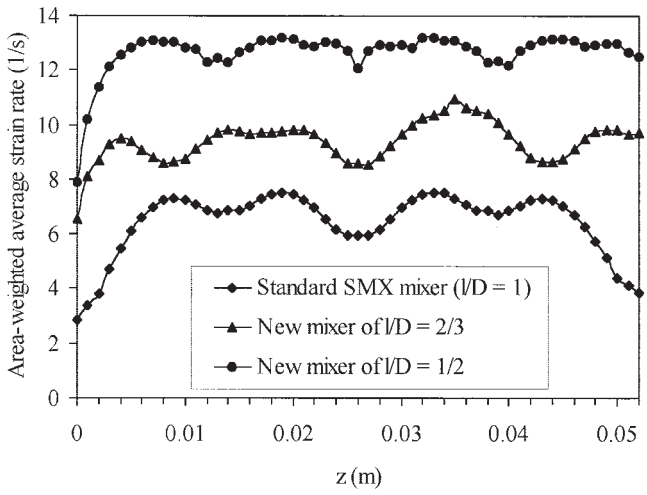

Figure 13. Area-weighted average strain rate on cross sections along *z*-axis for SMX and new designs.

smaller sample size are needed to further compare these two mixers.

Figure 15 shows a histogram of the maximum stretching efficiency, $e_{\lambda\,\max}$, with 17 bins of 0.025 from 0.4 to 0.825 for the three mixers. The relative volume fraction of $e_{\lambda\,\max}$ for three mixers is given. The mixer elements with reduced aspect ratio have a smaller volume fraction with predominantly elongational and squeezing flows and a greater volume fraction dominated by shear flow compared to those of the standard SMX static mixer because they have more solid surfaces in the mixing section. The relative volume fractions of $e_{\lambda\,\max} \geq 0.775$ for the mixer elements with $l/D = 1$, 2/3, and 1/2 are 11.4, 10.4, and 7.1%, respectively. These three mixers have the same volume-weighted average $e_{\lambda\,\max}$ of 0.692.

In the proposed reduced aspect ratio designs, the fluid elements are split and recombined more times, in comparison with the standard SMX mixer. Shorter mixing elements force periodic rotation (reorientation) of the fluid elements more often in the same length of mixing section. Denser arrangements of crossbars produce higher and more uniform strain rate. These characteristics produce a faster mixing rate and may benefit both distributive and dispersive mixing such as breakup of drops and particle clusters.

Conclusions

The effect of crossbar number (or width of crossbar) of SMX mixing elements on pressure drop and mixing was studied. The mixing element with 10 crossbars shows the best mixing quality based on particle tracking, followed closely by the standard SMX mixing element with eight crossbars. When the crossbar number is >10, the mixing quality dramatically worsens compared to scenarios with fewer crossbar numbers. New mixing elements with denser arrangement of crossbars and smaller aspect ratio than those of the standard SMX mixer produce higher strain rate and faster mixing rate.

Acknowledgments

The authors gratefully acknowledge the support of the Natural Sciences and Engineering Research Council of Canada (NSERC), Canadian Foundation for Innovation (CFI) and the Ontario Investment Trust (OIT) for research and equipment grants, which supported this research.

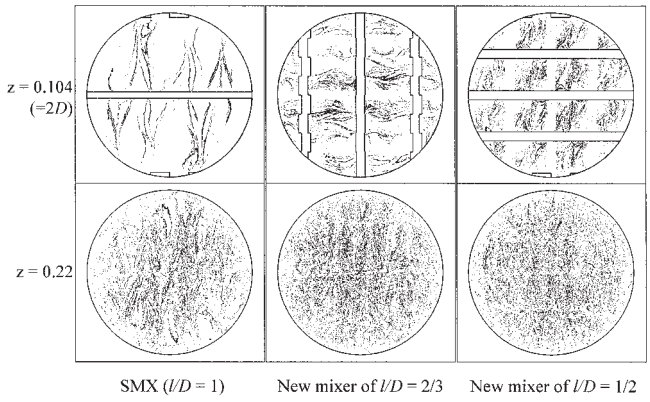

Figure 14. Particle positions on cross sections for the standard SMX mixer, the new mixer of l/D = 2/3, and the new mixer of l/D = 1/2.

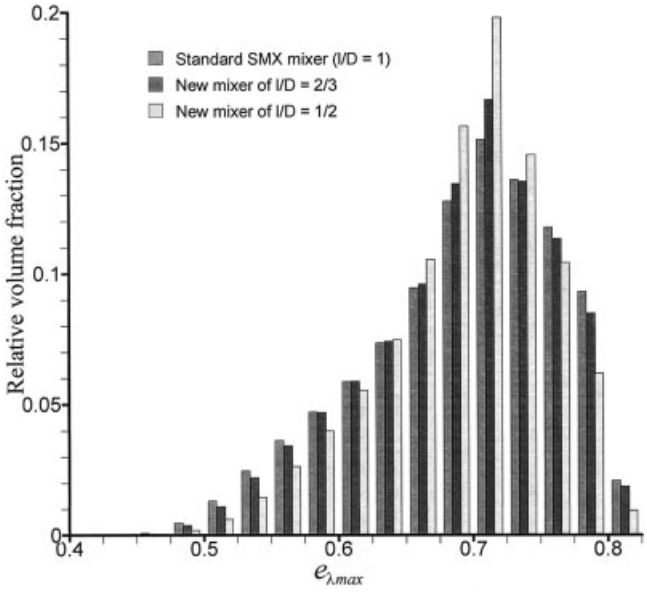

Figure 15. Histogram of the maximum stretching efficiency $e_{\lambda\,\max}$ for three mixers.

Notation

c_i = particle concentration in the ith sample
$\bar{c}$ = average particle concentration
COV = coefficient of variation
D = diameter of static mixer, m
$\mathbf{D}$ = the rate of deformation tensor, s^{-1}
$e_{\lambda\,\max}$ = maximum stretching efficiency
k = pressure drop ratio
l = length of a single mixing element, m
$\mathbf{n}_i$ = ith eigenvectors of $\mathbf{D}$
N = total sample number
P = pressure, Pa
ΔP_0 = pressure drop in empty tube, Pa
ΔP_{SM} = pressure drop in static mixer, Pa
v_x = x-velocity component, m/s
v_y = y-velocity component, m/s
x = x-coordinate
y = y-coordinate
z = z-coordinate

Greek letters

$\dot{\gamma}$ = strain rate, s^{-1}
λ = length stretch
λ_i = ith eigenvalue of $\mathbf{D}$
σ = standard deviation of particle concentration

Literature Cited

1. Shah NF, Kale DD. Pressure drop for laminar flow of non-Newtonian fluids in static mixers. *Chem Eng Sci*. 1991;46:2159-2161.
2. Li HZ, Fasol C, Choplin L. Pressure drop of Newtonian and non-Newtonian fluids across a Sulzer SMX static mixer. *Trans IChemE.* 1997;75:792-796.
3. Visser JE, Rozendal PF, Hoogstraten HW, Beenackers AACM. Three-dimensional numerical simulation of flow and heat transfer in the Sulzer SMX static mixer. *Chem Eng Sci.* 1999;54:2491-2500.
4. Streiff FA. Adapted motionless mixer design. Proc of Third European Conference on Mixing, Paper C2, University of York, England, April 4–6; 1979:171-188.
5. Pahl MH, Muschelknautz E. Static mixers and their applications. *Int Chem Eng.* 1982;22:197-205.
6. Allocca PT. Mixing efficiency of static mixing units in laminar flow. *Fiber Producer.* 1982;4:4-7.

7. Fleischli M, Wehrli M, Streiff FA, Lang E. Effect of diffusion and heat conduction on homogeneity in laminar static mixing. *Recents Prog Genie Proc.* 1997;11:283-290 (1997;51: Mixing 97: Recent Advances in Mixing).
8. Rauline D, Tanguy PA, Blevec JL, Bousquet J. Numerical investigation of the performance of several static mixers. *Can J Chem Eng.* 1998;76:527-535.
9. Rauline D, Blevec JL Bousquet J, Tanguy PAA. Comparative assessment of the performance of the Kenics and SMX static mixers. *Trans IChemE.* 2000;78:389-396.
10. Zalc JM, Szalai ES, Muzzio FJ, Jaffer S. Characterization of flow and mixing in an SMX static mixer. *AIChE J.* 2002;48:427-436.
11. Zalc JM, Szalai ES, Muzzio FJ. Mixing dynamics in the SMX static mixer as a function of injection location and flow ratio. *Polym Eng Sci.* 2003;43:875-887.
12. Mickaily-Huber ES, Bertrand F, Tanguy P, Meyer T, Renken A, Rys FS, Wehrli M. Numerical simulations of mixing in an SMRX static mixer. *Chem Eng J.* 1996;63:117-126.
13. Ottino JM. *The Kinematics of Mixing: Stretching, Chaos, and Transport.* Cambridge, UK: Cambridge Univ. Press; 1989.
14. Lai WM, Rubin D, Krempl E. *Introduction to Continuum Mechanics.* Elmsford, NY: Pergamon Press; 1974.
15. Bigio DI, Conner JH. Principal directions as a basis for the evaluation of mixing. *Polym Eng Sci.* 1995;35:1527-1534.
16. Liu S. *Laminar Mixing in an SMX Static Mixer.* PhD Thesis. Hamilton, ON, Canada: McMaster University; 2005.
17. Godfrey JC. Static mixers. In: Harnby N, Edwards MF, Nienow AW, eds. *Mixing in the Process Industries.* London, UK: Butterworth; 1985:239-243.

Manuscript received Dec. 23, 2004, and revision received May 24, 2005.